

Finite Element Simulation of Residual Stresses in Epitaxial Layers

Paweł Dłużewski¹, Grzegorz Jurczak¹, Grzegorz Maciejewski¹,
Sławomir Kret², Pierre Ruterana³ and Gerard Nouet³

¹ Full Institute of Fundamental Technological Research PAS, Świątokrzyska 21,
00-049 Warsaw, Poland

² Institute of Physics PAS, Al. Lotników 32/46, 02-668 Warsaw, Poland

³ ESCTM-CRISMAT UMR 6508 CNRS-ISMRA, 6 Boulevard du Maréchal Juin,
14050 CAEN Cedex, France

Keywords: Dislocations, Anisotropic Hyperelasticity, Residual Stresses

Abstract. A nonlinear finite element approach presented here is based on the constitutive equations for anisotropic hyperelastic materials. By digital image processing the elastic incompatibilities (lattice mismatch) are extracted from the HRTEM image of GaN epilayer. Such obtained tensorial field of dislocation distribution is used next as the input data to the FE code. This approach is developed to study the stress distribution associated with lattice defects in highly mismatched heterostructures applied as buffer layers for the optically active structures.

Introduction

It is well known that the strain field affects the properties of semiconductor devices [1]. By using the geometric phase method [2] to digital processing of High Resolution Transmission Electron Microscopy images (HRTEM) it is possible to determine the plain components of the lattice distortion field. The experimental details on the preparation of GaN epilayers on sapphire substrate considered here have been given in [3]. In the present paper a computational technique for predicting residual stresses induced by dislocations is discussed in brief. More details are given in [4]. Finite element (FE) method is rarely employed to predict the residual stress distribution induced by a tensorial field of dislocation distribution (DD). The reason of that yields from difficulties in finding of the suitable numerical algorithms based upon the displacement field method being the foundation of the most of FE codes. In the present paper we consider a nonlinear FE algorithm. The linear theory of elasticity is used very often mainly due to its efficiency in determination of analytical solutions. Thus, many analytical solutions for dislocation fields are available, see [5]. Nevertheless, the strains in epitaxial layers reach considerably larger values than in ordinary crystals. To hold a linear character of differential equations, the linear theory, by definition, ignores the nonlinear effects yielding from the differences between the actual and reference configurations of crystal lattice as well as from the asymmetry in the extension/compression response of real crystals, see [6].

Kinematics

Let \mathbf{X} denote a reference position of a given material particle which after deformation takes a new position \mathbf{x} . In such a case the motion is described by the material mapping $\mathbf{x} = \mathbf{x}(\mathbf{X}, t)$ where t denotes time. In the Euclidean space the deformation gradient and displacement gradient are related each other by the following equation

$$\mathbf{F}^{-1} = \frac{\partial \mathbf{X}}{\partial \mathbf{x}} = \mathbf{1} - \nabla \mathbf{u}, \quad (1)$$

where $\nabla \mathbf{u} \stackrel{\text{df}}{=} \frac{\partial \mathbf{u}}{\partial \mathbf{x}}$.

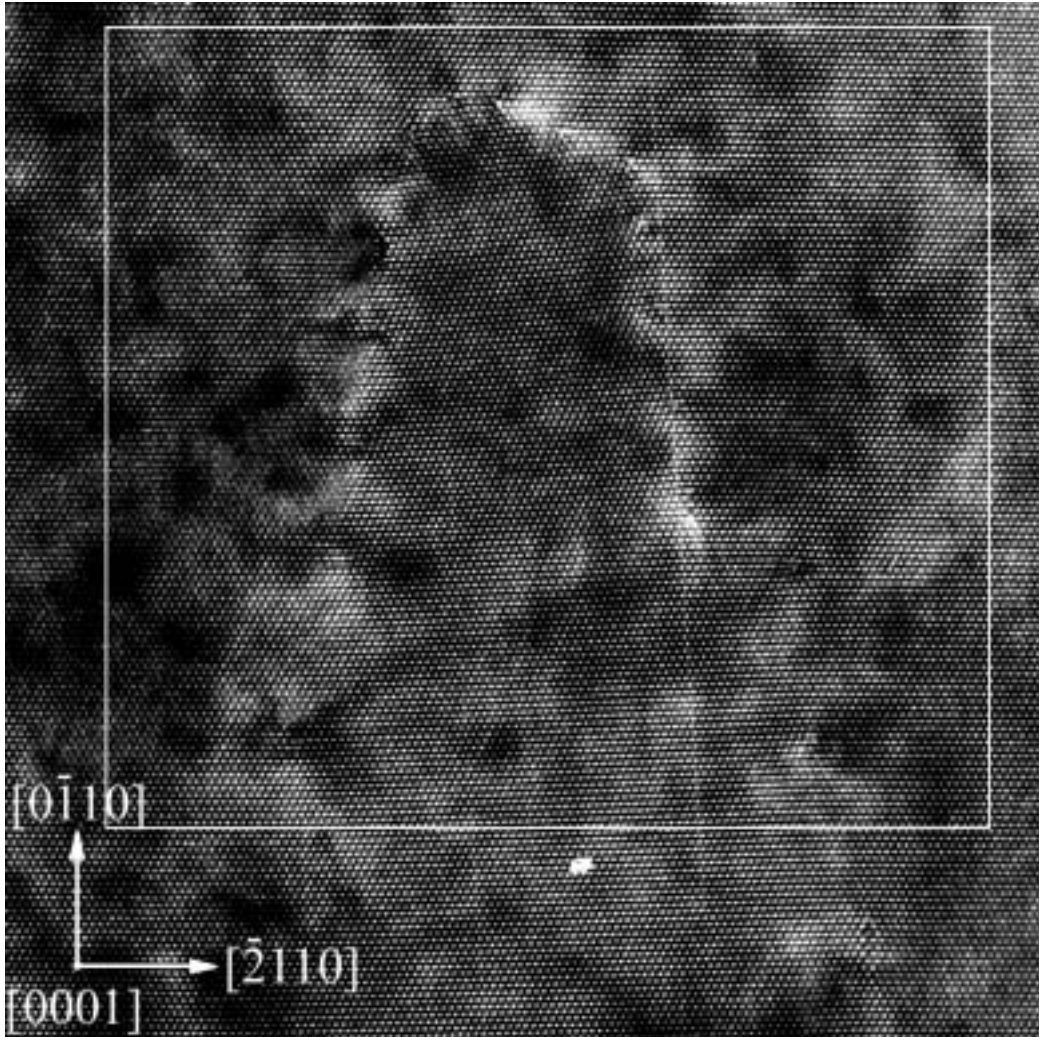


Fig. 1. HRTEM image of treating dislocations $1/3\langle \bar{2}110 \rangle$ in the GaN layer deposited on sapphire.

By means of the geometric phase method the distribution of lattice distortions can be reconstructed from the HRTEM image. The method is based upon centering a small aperture around a strong reflection in the Fourier transform of image [2]. The phase components of the resulting complex image give information about local displacements of atomic planes. Applying two non-collinear Fourier components a two-dimensional piecewise continuous elastic displacement field $\hat{\mathbf{u}}(\mathbf{x})$ is extracted from the HRTEM image. Such obtained a piece-wise field holds the same left- and right-handed derivatives on the discontinuity lines. Therefore, differentiating the displacement field a continuous field of lattice distortions $\beta(\mathbf{x})$ is reconstructed

$$\beta = \frac{\partial \hat{\mathbf{u}}}{\partial \mathbf{x}}. \quad (2)$$

More details on determination of the distortion field are given in [7]. It is easy to prove that using the distortion tensor field $\beta(\mathbf{x})$, we can recover the components of the so-called true Burgers vector according to the relation

$$\hat{\mathbf{b}} = \oint_c \beta \, dx, \quad (3)$$

where c denotes the Burgers circle in the actual configuration.

In the present approach we assume a multiplicative decomposition of the deformation gradient

$$\mathbf{F} = \underbrace{\mathbf{R}\mathbf{U}\mathbf{F}_{pl}}_{\mathbf{F}_{lt}}, \quad (4)$$

where \mathbf{R} , \mathbf{U} , \mathbf{F}_{lt} and \mathbf{F}_{pl} denote, respectively, the rotation and stretch of crystal structure determined in relation to its local relaxed (intermediate) configuration, the lattice deformation gradient and a remnant (plastic deformation) resulting from the (permanent) rearrangement of atoms composing the crystal lattice. \mathbf{F}_{lt} can be specified [4] as

$$\mathbf{F}_{lt} = (\mathbf{1} - \boldsymbol{\beta})^{-1}. \quad (5)$$

The local distributions of the true Burgers vectors referred to the lattice reference configuration are described by the following DD tensor

$$\hat{\boldsymbol{\alpha}} = \text{curl} \mathbf{F}_{lt}^{-1} \mathbf{F}_{lt}^{-T} \det \mathbf{F}_{lt}. \quad (6)$$

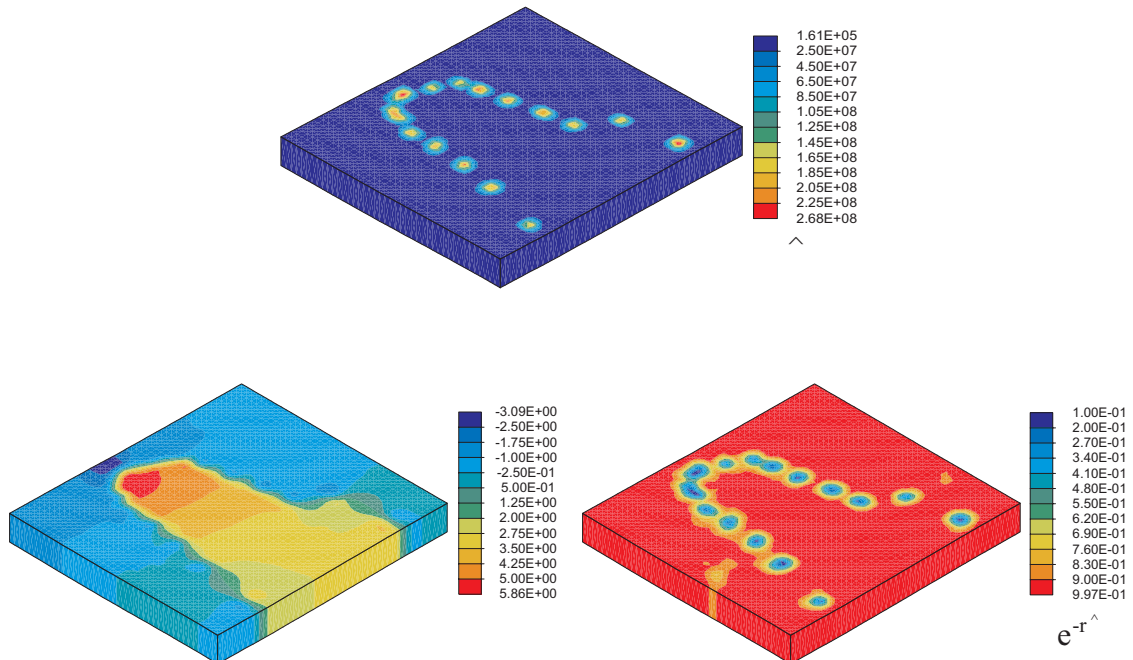


Fig. 2. Fields of the DD tensor invariant $\hat{\boldsymbol{\alpha}}(\mathbf{x})$, lattice orientation $\varphi(\mathbf{x})$ and elastic stiffness reduction factor $e^{-r\hat{\boldsymbol{\alpha}}}$ for $r=60$.

Constitutive model

In the computational model we assume the stiffness reduction in lattice disordered regions according to the relation

$$\hat{\mathbf{c}}_{\alpha} = e^{-r\hat{\boldsymbol{\alpha}}} \hat{\mathbf{c}}, \quad (6)$$

where $\hat{\mathbf{c}}$ is the elastic stiffness tensor corresponding to a perfect lattice and r is a scalar parameter. The tensorial field of DD $\hat{\boldsymbol{\alpha}}$ allows the computer recognition of dislocation core region during the computational process. The lattice disordered regions are recognized by using the following invariant of the DD tensor

$$\hat{\alpha} = \sqrt{\hat{\alpha}_{xz}^2 + \hat{\alpha}_{yz}^2}. \quad (7)$$

Dislocation core regions give strongly localized peaks on the DD tensor field, see $\hat{\boldsymbol{\alpha}}(\mathbf{x})$ in Fig. 2. In the mentioned figure it is also shown how far the scalar parameter $r=60$ induces the elastic stiffness reduction in

dislocation core regions, see $e^{-r\alpha}$. With respect to numerical problems we have limited the stiffness reduction in dislocation cores to 0.1c.

Supposing that the specific strain energy satisfies

$$\psi(\hat{\boldsymbol{\varepsilon}}) = \frac{1}{2\hat{\rho}} \hat{\mathbf{c}}_{\alpha}^{ijkl} \hat{\varepsilon}_{ij} \hat{\varepsilon}_{kl}, \quad (9)$$

where $\hat{\boldsymbol{\varepsilon}} \stackrel{\text{df}}{=} \frac{1}{m}(\mathbf{U}^m - \mathbf{1})$, $\hat{\rho}$ is the mass density in the reference configuration. It can be proved that the Cauchy stress is governed by the following equation [6]

$$\boldsymbol{\sigma} = \mathbf{R}(\hat{\boldsymbol{\Lambda}} : \hat{\mathbf{c}}_{\alpha} : \hat{\boldsymbol{\varepsilon}}) \mathbf{R}^T \det \mathbf{F}^{-1}. \quad (10)$$

The fourth-order tensor $\hat{\boldsymbol{\Lambda}}$ decomposed in the strain eigenvector basis $\{\hat{\boldsymbol{\varepsilon}}_I\}$ is represented by the following non-vanishing components

$$\hat{\Lambda}_{IIII} = \hat{\Lambda}_{IIII} = \delta_{II} \quad \text{for } \hat{\boldsymbol{\varepsilon}}_I = \hat{\boldsymbol{\varepsilon}}_I, \quad (11)$$

$$\hat{\Lambda}_{IIII} = \hat{\Lambda}_{IIII} = \frac{2(\hat{\boldsymbol{\varepsilon}}_I - \hat{\boldsymbol{\varepsilon}}_J)}{e^{\hat{\boldsymbol{\varepsilon}}_I - \hat{\boldsymbol{\varepsilon}}_J} - e^{\hat{\boldsymbol{\varepsilon}}_J - \hat{\boldsymbol{\varepsilon}}_I}} \quad \text{for } \hat{\boldsymbol{\varepsilon}}_I \neq \hat{\boldsymbol{\varepsilon}}_J, \quad (12)$$

where $\hat{\boldsymbol{\varepsilon}}_I$ is the I-th eigenvalue of $\hat{\boldsymbol{\varepsilon}}$.

Finite element method

FE algorithm developed here is based on the integration of the equilibrium equation over the current configuration, cf. [4]. The following differential equation is integrated

$$\text{div} \boldsymbol{\sigma} = 0, \quad (13)$$

where the Cauchy stress tensor is a nonlinear function of \mathbf{u} , $\nabla \mathbf{u}$, $\boldsymbol{\beta}$ and $\nabla \boldsymbol{\beta}$. In such a case, due to the nonlinear geometry the constitutive model applied gives the nonsymmetric tangent stiffness matrix. We have assumed the following vector of nodal variables $[\mathbf{a}] = [\mathbf{u} \quad \hat{\boldsymbol{\beta}}]$, where

$$\hat{\boldsymbol{\beta}} = (\mathbf{1} - \boldsymbol{\beta})^{-1} - \mathbf{1}. \quad (14)$$

Due to the complex dependence of the residuum on $[\mathbf{a}]$ the tangent stiffness matrix was calculated numerically as

$$\mathbf{K}_{ij} \approx \int_{\mathbf{v}} \nabla N_i \frac{\partial [\boldsymbol{\sigma}(\mathbf{a}) \det \mathbf{F}]}{\partial \mathbf{a}_j} \det \mathbf{F}^{-1} d\mathbf{v}. \quad (15)$$

More details of this FE approach have been given in [8].

Numerical example. In order to illustrate the method let us consider a selected area of GaN, see Fig. 1. The HRTEM image is a 2D projection of the real 3D structure with edge dislocations. By the digital image processing the distortion field of the crystal lattice is obtained in the form of four plain components $\hat{\boldsymbol{\beta}}(x,y)$. To reconstruct distortions in z-direction we assumed at the beginning that for all z-coordinates the source distortions hold the constraints $\hat{\boldsymbol{\beta}}(x,y,z) = \hat{\boldsymbol{\beta}}(x,y)$. Nevertheless, during computational process the dimensions of finite elements changed due to two reasons: (1) initial deformation - imposed by the source distortions and (2) elastic relaxation - due to elastic response proper to the assumed hyperelastic material and boundary condition. The second reason induces for example the stress relaxation in the z-direction especially on the external stress-free surfaces of the FE mesh.

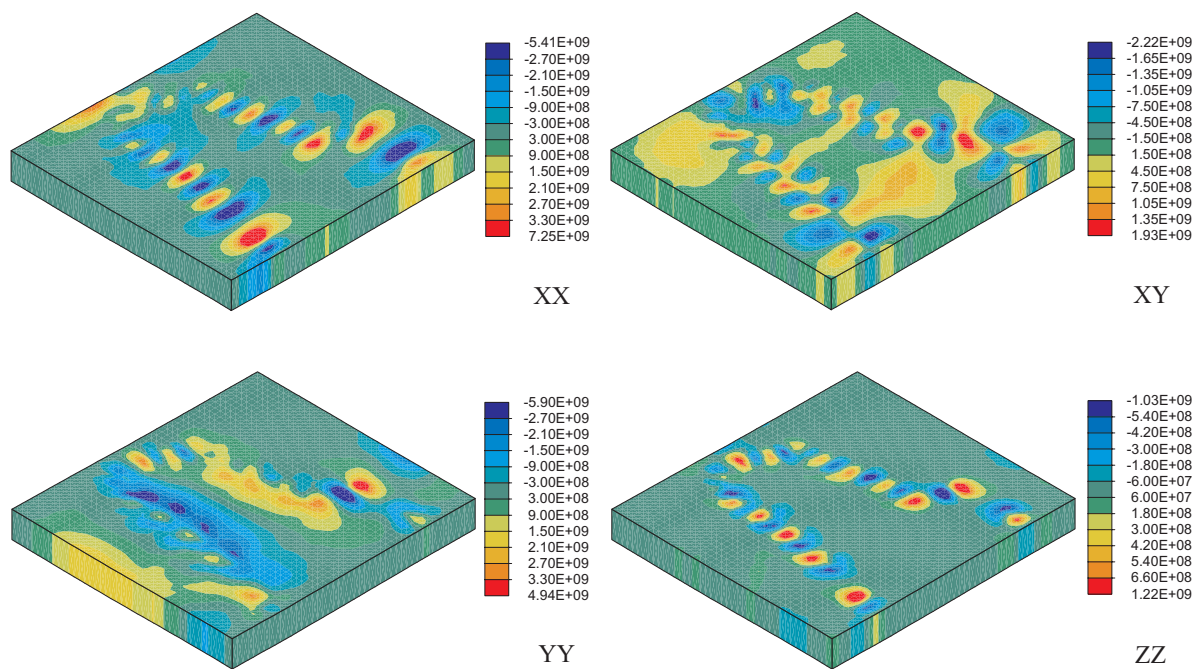


Fig. 3. The Stress distribution in GaN layer, the mid-cross section through FE mesh.

Each of finite elements had the following initial dimensions $7.2874 \text{ nm} \times 7.2874 \text{ nm} \times 72.874 \text{ nm}$. The values of the parameters r and m were assumed to be 60 and -3, cf. [9] and [4], respectively. Full (3D) second-order elastic anisotropy was included to the analysis. The stiffness constants were taken after Takagi [10]: $C_{11} = 374$, $C_{12} = 106$, $C_{13} = 70$, $C_{33} = 379$, $C_{44} = 101$ GPa. The finite element calculation has been performed by using an anisotropic hyperelastic FE element implemented to the Taylor's FEAP program as a user element adopted to read lattice distortion field extracted directly from the HRTEM image. The boundary-value problem for the stress equilibrium was solved by using the modified Newton-Raphson method. The numerical results obtained for the residual Cauchy stress distribution are shown in the 3D view of the mid-plane cross section of the FE mesh, see Fig. 3.

Summary

The residual stresses have been obtained here as a solution of the boundary-value problem stated for residual stresses induced by the DD tensor field extracted from the HRTEM image of the GaN epilayer. Using both the geometric phase method, continuum theory of dislocations and theory of anisotropic hyperelastic materials the components of the stress field have been calculated. This method links the digital processing of the HRTEM images with the object oriented FE method, where the output data obtained from the image processing are used as the input data to the nonlinear FE analysis.

Acknowledgment

This research was supported by the State Committee for Scientific Research (KBN) in Poland under Grant No. 7 T07A 015 17.

References

- [1] B.R. Nag: *Physics of Quantum Well Devices* (Solid-State Sci. Techn. Lib. Kluwer Academic Publ. 2000).
- [2] M.J. Hÿtch, E. Snoeck, and R. Kilaas: *Ultramicroscopy* Vol. 74 (1998), p. 131.
- [3] S. Kret, P. Dłuzewski, G. Maciejewski, V. Potin, J. Chen, and P. Ruterana: The dislocation of low-angle grain boundaries in GaN epilayers: a HRTEM quantitative study and finite element stress state calculation. Accepted for publication in *Diamond and Related Mater.* (2001).
- [4] P. Dłuzewski, G. Maciejewski, G. Jurczak, and S. Kret: Nonlinear analysis of residual stresses induced by misfit dislocations in epitaxial layers. Submitted to *J. Mech. Phys. Solids* (2001).
- [5] J. P. Hirth and J. Lothe: *Theory of Dislocations* (Wiley, New York 1982).
- [6] P. Dłuzewski: *J. Elasticity* Vol. 60 (2000), p.119.
- [7] S. Kret, P. Dłuzewski, P. Dłuzewski, and J.Y. Laval: On the measurement of dislocation cores distribution in GaAs/ZnTe/CdTe heterostructure by transmission electron microscopy. Submitted to *Phil. Mag. A* (2001).
- [8] P. Dłuzewski, G. Jurczak, and H. Antúnez: Logarithmic measure of strains in finite element modelling of anisotropic deformations of elastic solids. Accepted for publication in *Computer Assisted Mechanics and Engineering Science* (2003).
- [9] A.J. Foreman, M.A. Jaswon, and J.K. Wood: *Proc. Phys. Soc. A* Vol. 64 (1951), p. 156.
- [10] Y. Takagi, M. Ahart, T. Azuhata, T. Sota, K. Suzuki, and S. Nakamura: *Physica B* Vol. 219-220 (1996), p. 547.